

# Differential Relay with Adaptation during Saturation Period of Current Transformers

Waldemar Rebizant

Wroclaw University of Technology  
Wybrzeze Wyspianskiego 27  
50-369 Wroclaw, Poland  
rebizant@pwr.wroc.pl

Kurt Feser, Tammam Hayder

University of Stuttgart  
Pfaffenwaldring 47  
70569 Stuttgart, Germany  
thayder@ieh.uni-stuttgart.de

Ludwig Schiel

SIEMENS AG Berlin  
Wernerwerkdammm 5  
13623 Berlin, Germany  
ludwig.schiel@siemens.com

**Abstract**—A new adaptive approach to differential protection of generators and transformers for fault cases with CT saturation due to DC component is presented. Improved stabilization for external faults is achieved by appropriate temporal adjustment of the differential curve for the time period of CT saturation. All necessary algorithms needed to implement the adaptation, i.e. measurement of current signal parameters, assessment of CT saturation time and determination of needed adaptation grade are described. The protection developed was tested with both EMTP-generated and real world registered current signals.

**Index Terms** – adaptivity, CT saturation, differential protection, digital signal processing, synchronous machine, transformer.

## I. INTRODUCTION

**D**IFFERENTIAL principle belongs to the most commonly accepted ones for protection of generators and transformers against internal faults. Current or impedance stabilized relays are usually applied. The differential current  $I_d$  resulting from signals at both sides of the protected plant is compared with the through current  $I_s$ . It is checked whether the operating point in the  $I_s$ - $I_d$  plane moves to the trip region above the stabilizing curve, which leads to relay pick-up and switching off the protected plant.

Even though the differential relays are considered quite reliable and robust, there are situations when they may malfunction. Contradictory requirements of high sensitivity and selectivity can not reconcile in cases of faults with small through currents which may evoke over-tripping if the CTs saturate due to content of DC component with high value of decaying time constant. Such conditions may arise e.g. during external faults close to generator-transformer units when the time constant  $T_N$  is as high as 200-300ms. Sample signals observed during such faults are shown in Fig. 1. Contrary to high amplitude faults when the CTs saturate within first half-cycle or full-cycle of the current signal after fault inception, the saturation effects for DC-induced cases appear only few cycles later and have somewhat different nature. One can observe that the negative half of the signal wave is also falsely transformed to the CT secondary side. Detailed

analyses of the saturation phenomena are not presented in the paper due to space limitation.

In Fig. 2 the calculated amplitudes of differential and through currents are presented both as time-varying signals and in form of a trajectory in the differential plane. The through current  $I_s$  is quite small in this case which, by relatively high differential signal, makes the current trajectory pass through the differential curve to the trip region. In Fig. 2a the relay output signal is plotted additionally showing that under conditions described the relay would trip appr. 2.5 cycles after fault inception. That means relay maloperation (over-tripping) occurs which may bring undesired costs of tripping-off the generator and loss of supply to some of the customers in the network.

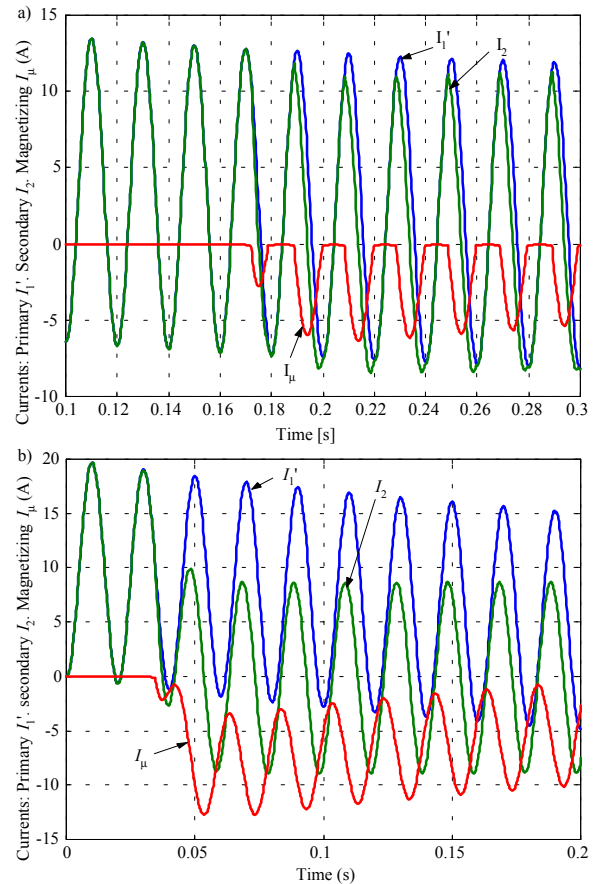


Fig. 1. Primary, secondary and magnetizing currents of a CT during a generator-close fault: a)  $I_1=2I_n$ ,  $I_{DC}=0.5I_1$ ,  $T_N=300$ ms, b) same as in a) but for  $I_{DC}=I_1$ .

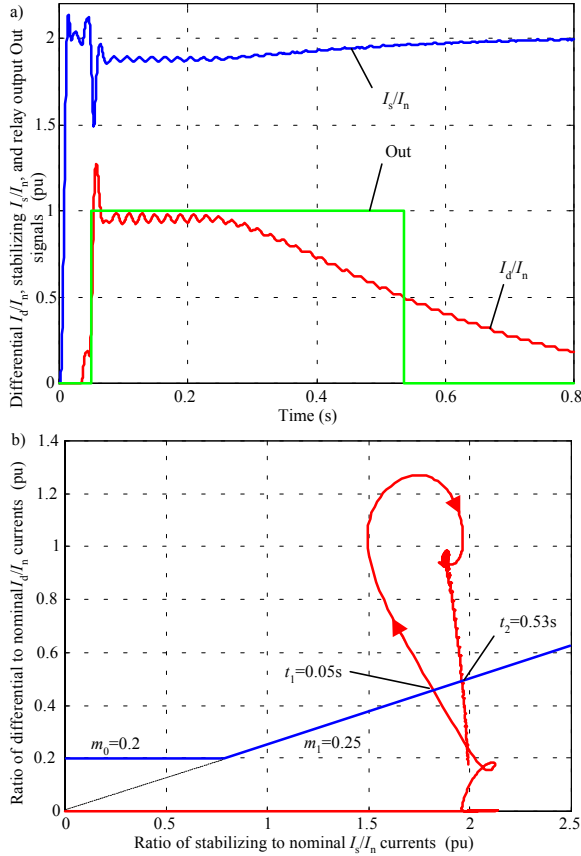


Fig. 2. Differential and stabilizing currents: a) signals in time domain (Out – relay tripping signal), b) trajectory at the differential plane;  $I_1=2I_n$ ,  $I_{DC}=I_1$ ,  $T_N=300$ ms.

The stabilization applied (set typically at  $m_0=0.2$  and  $m_1=0.25$ , see Fig. 2b) is good enough for the cases of external faults with high current amplitudes. In the cases described above, however, the stabilization level is not sufficient to prevent the relay from undesired tripping.

In the paper the idea of adaptive differential relay is presented with the aim of avoiding tripping for external faults with small through currents accompanied with CT saturation due to DC component. In the following chapters the general idea of adaptive protection together with the detailed information on the algorithms of current parameter estimation, CT operation prediction and determination of the necessary adaptation degree are described. The results of application of the new adaptive method are compared with the ones obtained with traditional non-adaptive approach.

## II. ADAPTIVE DIFFERENTIAL PROTECTION

### A. Block scheme of the adaptive protection

The idea of adaptivity with reference to the differential protection is summarized in Fig. 3. The procedure of adaptive adjusting of the differential characteristic consists of the following steps:

- Calculation of the initial value (amplitude)  $I_{DC}$  and time constant  $T_N$  of the decaying DC component as well as the amplitude of the current fundamental

frequency component  $I_1$  for the time instant just after fault inception,

- Determination (prediction) of the flux density value  $B_s$  leading to CT saturation, maximal expected flux density level  $B_{max}$  in the CT core and comparison of the values,
- Calculation of the expected CT saturation period, i.e. time instants  $t_{s1}$  and  $t_{s2}$  of saturation beginning and fizzling out,
- Determination of the necessary level of adaptation for given fault case (shifting up of the differential curve or slope changing of the stabilizing section),
- Measurement of the through current amplitude values (differential curve adjusting takes place for fault currents close to nominal ones, i.e. up to  $3I_n$ ),
- Execution of the on-line adaptation of the differential curve for the time period  $[t_{s1}, t_{s2}]$ .

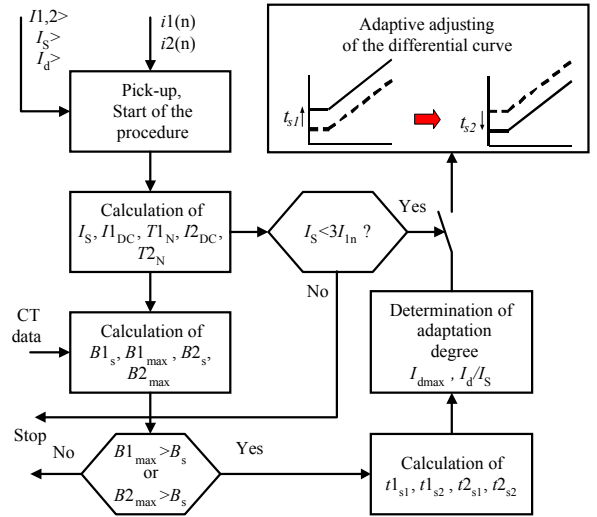


Fig. 3. Block scheme of the adaptive protection.

It is worth to notice that the calculation of mentioned above values is performed for the signals from CTs at both sides of the protected plant (big indexes 1, 2 – Fig. 3). The adaptation is carried into effect at or slightly before the predicted time instant of CT saturation (earlier from both calculated values is accepted for this purpose).

### B. Measurement of DC component parameters

Various algorithms have been examined for calculation of DC component parameters, i.e. its amplitude  $I_{DC}$  and time constant  $T_N$ . The latter value is a complex function of the generator, network and fault data. Both parameters are further used as input data for the adaptive protection procedure described.

In the literature the following methods for DC component filtering (rejection) and/or measurement can be found:

- Filtering (rejection) of decaying DC component (with only coarse or without measurement of its parameters) is often performed with application of band-pass or high-pass filters of FIR type [4] (non-

recursive filters having sine and cosine data windows or just a cosine filter) or the so called mimic filters [5].

- Least error squares based methods [6] in recursive or non-recursive versions are also used to filter out the DC component that is either taken or not taken into consideration as a part of the signal model.
- State space algorithms, where the DC component is considered as one of the state variables, have a special mixed rejection-measurement character; examples of the algorithms of this kind are the state observer and the Kalman filter [7, 8], with a common weakness related to the necessity of knowing the statistical features of the signal to be measured and its expected noises.
- Algorithms for elimination and partial measurement of the DC component based on the assumption of a detailed signal model and modified half- or full-cycle filters (Fourier or Walsh functions) [9, 10, 11].

After thorough analysis concerning accuracy and dynamics of measurement the method described in [11] with certain modifications has been accepted for further use. The algorithm proposed is based on full-cycle averaging of the current which corresponds to signal filtering with the 0-th order Walsh filter. In recursive form the averaging algorithm can be expressed as

$$i_{w0}(k) = i_{w0}(k-1) + wal_0(k)[i(k) + i(k-N)]. \quad (1)$$

Coefficient  $r$  dependent on the decaying DC time constant is further calculated as a quotient of the last and preceding values of the averaged current signal

$$r(k) = \frac{i_{w0}(k)}{i_{w0}(k-1)}. \quad (2)$$

The sought value of time constant  $T_N$  is then obtained from the following equation

$$T_N = \tau = \frac{T_p}{\ln[r(k)]}, \quad (3)$$

$T_p$  – sampling period,

while the initial value of DC component is calculated from:

$$I_{DC} = \frac{i_{w0}(k)}{\sum_{n=0}^{N-1} r(k-n)^n} e^{kT_p}. \quad (4)$$

with the exponential factor introduced for correction of time passing ( $k$  sampling periods counted from the fault inception). Accurate measurement results are here guaranteed when  $k=N+1$  current samples after fault inception are available.

It is worth to mention that significant improvement of the measurement accuracy for the fundamental

frequency component amplitude is obtained when the calculated DC component is subtracted from the signal before actual measurement, according to:

$$i_f(k) = i(k) - I_{DC} e^{-kT_p/T_N}. \quad (5)$$

### C. CT saturation prediction

The problems related to quality (accuracy) of primary current transformation to the secondary side of conventional CTs during severe saturation of their core have already been described in several papers, e.g. [2], [3], as well as in international standards [1]. The relationships given below originate from the references mentioned, with certain modifications introduced by the authors of this paper to match them to the saturation phenomena due to DC component.

The estimation of CT saturation starting time ( $t_{s1}$ ) can be done with use of one of the following three relationships:

- a) Non-linear formula for the magnetic flux density  $B_s$  at the beginning of saturation period [2]

$$B_s = \frac{\mu w_2 I_2}{l} \left( \frac{T_N}{T_W - T_N} (e^{-t_{s1}/T_W} - e^{-t_{s1}/T_N}) \right), \quad (6)$$

solvable for the time  $t_{s1}$  e.g. with the least error squares method. Herein are

$\mu$  – magnetic permeability of the iron core,

$w_2$  – number of turns of the secondary winding,

$l$  – middle length of magnetic force lines in the CT iron core,

$I_2$  – amplitude of the secondary current (fundamental frequency component),

$T_W$  – CT time constant,

$T_N$  – time constant of the network seen from the fault point.

- b) Simplified version of (6), with CT time constant  $T_W$  assumed as infinite (significantly higher as the network time constant  $T_N$ ), in the form

$$t_{s1} = -T_N \cdot \ln \left( 1 - \frac{B_s \cdot q}{T_N \cdot R_2 \cdot I_2} \right), \quad (7)$$

- c) Formula proposed in IEEE Standard C37.110-1996 [1]:

$$t_{s1} = \frac{-(X/R)}{2\pi f} \cdot \ln \left( 1 - \frac{K_s - 1}{(X/R)} \right) = -T_N \cdot \ln \left( 1 - \frac{K_s - 1}{\omega T_N} \right), \quad (8)$$

with  $K_s = \frac{V_{sat}}{I_2 \cdot (R_2 + R_s + Z_b)}$  – saturation factor,

$X, R$  – reactance and resistance of the network at the fault spot,

$R_2$  – resistance of the CT secondary winding,

$R_s$  – resistance of the leads,

$Z_b$  – apparent impedance of the CT burden.

From the magnetic flow law

$$B_s = \frac{\mu}{l} w_2 i_s', \quad (9)$$

by  $i_s = I_{DC} e^{-t_{s2}/T_N}$  (neglect of ampere turns due to fundamental frequency current), one can derive a formula for the CT saturation end time ( $t_{s2}$ ) in the form

$$t_{s2} = T_N \ln \left( \frac{\mu w_2 I_{DC}'}{l B_s} \right). \quad (10)$$

The flux density value  $B_s$  leading to CT saturation and the maximal expected flux density level  $B_{max}$  in the CT core can be determined as [3]

$$B_s = \frac{\mu}{l} \frac{w_1 K_n I_{n1}}{\omega T_W}, \quad (11)$$

$$B_{max} = \frac{\mu}{l} w_2 I_2 \left[ \left( \frac{T_N}{T_W} \right)^{\frac{T_W}{T_W - T_N}} + \frac{1}{\omega T_W} \right], \quad (12)$$

whereas the time constant  $T_W$  can be calculated from the CT parameters as follows

$$T_W = \frac{L_W}{R_W} = \frac{L_0 + L_s + L_b}{R_2 + R_s + R_b}. \quad (13)$$

When the effective CT iron core cross-section  $q$  and middle length of magnetic force lines  $l$  in the core are known the value of  $T_W$  can be determined from

$$T_W = \frac{w_2^2 q \mu}{l R_W}. \quad (14)$$

Needless to say, the application of the above-presented formulae is possible in dependence on the availability of the CT and network parameters. Introductory analyses and simulative investigations have shown that the values obtainable with formula (7) are very close to those resulting from simulation of CT operation and real-world recordings. The outcomes of equation (8) are usually underestimated, i.e. smaller than in reality. That means the IEEE standard formula delivers rather conservative values of  $t_{s1}$ , being (in our case) situated on the right side in the sense of eventual adaptation being realized somewhat earlier than really required. On the other hand, the formula (8) is the only one that may be applied in the cases when precise data on required CT parameters is not available.

#### D. Adaptation versions and level

The design of the adaptive differential protection included also research on appropriate versions and

level of adaptation. Adaptive adjusting of the differential characteristic may be realized according to one of the following scenarios (illustrated in Fig. 4):

- shifting up the stabilizing curve before the saturation begins, then shifting it down to the standard position after CT saturation disappeared (Fig. 4a),
- changing the slope  $m_1$  of the differential curve (stabilizing section) to a higher value, then return to standard settings (Fig. 4b),
- forming an additional transitory restraining area above the stabilizing curve of e.g. polygonal shape (covering the area of foreseeable location of current trajectory), then removing the area (Fig. 4c),
- blocking of the entire relay for the CT saturation time period.

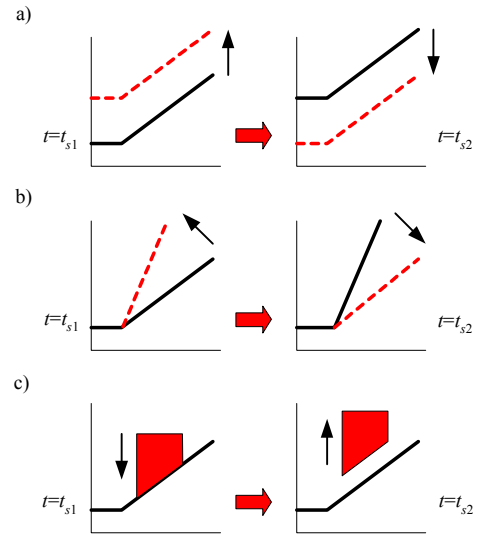


Fig. 4. Conceivable versions of adaptive adjusting of the differential curve: a) vertical shifting, b) slope change, c) additional restraining area.

Independent of the adaptation version that would be applied, additional research on determination of the optimal adaptation grade is to be done. All the important variables and coefficients influencing the expected level of differential and stabilizing currents are to be taken into account, such as already calculated parameters of DC component, amplitude of the fundamental frequency component and the estimated time instants of expected CT saturation beginning and fizzling out. Since adjusting of the differential curve is to be done before CT saturation begins, i.e. when the amplitudes of maximal differential and through currents are not known yet, one needs to derive the relationships enabling prediction of the maximal expected ratio  $I_d/I_s$ , and indirectly the localization of relay operation point in the  $I_d=f(I_s)$  plane.

After thorough simulative investigations the empirical formulae for the variables to be predicted as functions of the already measured values of  $I_1$ ,  $I_{DC}$ ,  $T_N$ ,  $t_{s1}$  and  $t_{s2}$  have been found. The expected values of

$I_{dmax}$  and ratio  $I_d/I_s$ , in dependence on CT saturation beginning  $t_{s1}$  or saturation duration  $t_{s2}-t_{s1}$ , can be calculated as follows

$$I_{dmax} \cong \frac{1}{25T_N t_{s1}}, \quad (15)$$

$$I_{dmax} \cong \frac{(t_{s2}-t_{s1})^2(4-I_{DC}/I_1)}{10T_N}, \quad (16)$$

$$\frac{I_d}{I_s} \cong \frac{3I_{DC}}{I_1}(t_{s1}-0,6), \quad (17)$$

$$\frac{I_d}{I_s} \cong (\frac{5}{9}I_{DC}/I_1+0,2)(t_{s2}-t_{s1}-0,3). \quad (18)$$

The relationships (15) and (16) can be used to assess the expected level of differential current amplitude, which defines required range of shifting up the differential curve (adaptation version a)). With the formulae (17) and (18) the expected ratio  $I_d/I_s$  is determined, which may be applied as a guideline for setting new value of the stabilizing slope  $m_1$ . For selectivity reasons it is proposed to define the new settings multiplying the values from (15) – (18) with an additional safety factor from the range 1.15 – 1.20.

The upper limit of the expected value of the ratio  $I_d/I_s$  can also be assessed with the following simple formula being only a function of the calculated current signal parameters

$$m_1 = \frac{I_d}{I_s} \cong 0,8 \frac{I_{DC}}{I_1}. \quad (19)$$

More details on the above-described results will be presented in other papers.

### III. RELAY TESTING

The developed and described above adaptive protection relay has been tested with simulation and real-world recorded fault signals. Below one chosen example of its operation for a real external fault is presented. The fault occurred close to generator terminals and was accompanied with DC induced CT saturation.

In Fig. 5 the current signals from both sides of the protected generator (secondary signals, phase L1) are shown with additionally superimposed DC component. One can see that the DC parameters (calculated according to (3) and (4)) are found quite correctly, since the DC curve follows closely the maxima of current waveforms, especially for the time period before CT saturation for which the values were determined. Higher values from those calculated for currents at both generator sides ( $T_N=114,5ms$ ,  $I_{DC}=1,7A$ ,  $I_1=3,89A$ ) were taken as input variables for calculations at further adaptation steps.

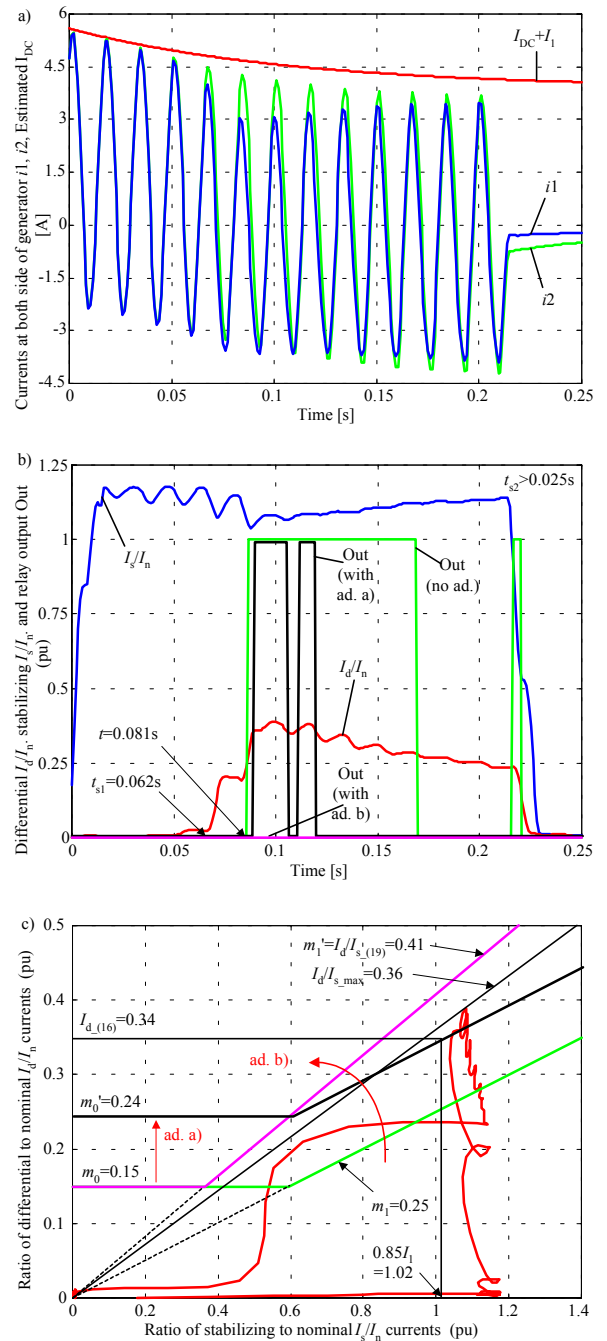


Fig. 5. Operation of the proposed adaptive differential protection for a real-world registered external fault case: a) current signals and estimated DC component, b) differential and stabilizing currents, protection output signals, c) adaptive adjustment of the differential curve in the  $I_d=f(I_s)$  plane.

The effects of adaptive adjusting of the differential curve can be seen in Fig. 5b and 5c. Appropriate changes (version a) – shifting up, version b) – setting new value of the stabilizing slope) were introduced at time instant  $t_{s1(7)}=62.3ms$ , i.e. before the non-adaptive relay picks up (curve Out (no ad.) in Fig. 5b). The calculated end-of-saturation time  $t_{s2(10)}=363ms$  was greater than the time range presented in Fig. 5. The adaptation by shifting up (version a) was not effective enough in the considered case, the differential curve shifting was too small and the relay picked up. The newly set stabilizing slope (version b)), on the

contrary, has fulfilled the expectations, i.e. the stabilization conditions have been significantly improved and unwanted tripping for the external fault was avoided.

#### IV. CONCLUSIONS

In the paper a new adaptive concept and detailed algorithms of differential protection for synchronous machines and transformers are presented. The protection developed offers improved stabilizing features for external fault cases with CT saturation evoked by DC component with high decaying time constant. The protection proposed has been tested with EMTP-generated current signals as well as real-world recordings, having proved better operation than standard solutions without adaptation.

#### V. ACKNOWLEDGEMENT

The first author gratefully acknowledges financial support from the Alexander-von-Humboldt Foundation (financing of his research stay at the University of Stuttgart, Germany, Sept.-Dec. 2003).

#### VI. REFERENCES

- [1] ANSI/IEEE C37.110 Standard: IEEE Guide for the application of current transformers used for protective relaying purposes.
- [2] A. Fischer and G. Rosenberger, "Verhalten von linearen und eisengeschlossenen Stromwandler bei verlagerten Kurzschlußströmen", *Elektrizitätswirtschaft*, Jg. 67 (1968), Heft 12, pp. 310-315.
- [3] A. Wiszniewski, *Przekładniki w elektroenergetyce*, WNT, Warszawa, wyd. I - 1982, wyd. II - 1992.
- [4] A.G. Phadke and J.S. Thorp, *Computer relaying in power systems*, John Wiley & Sons Inc., 1988.
- [5] G. Benmouyal, "Removal of DC-offset in current waveforms using digital mimic filtering", *IEEE Transactions on Power Delivery*, Vol. 10, No. 2, April 1995, pp. 621-628.
- [6] M. Sachdev and M. Nagpal, "A recursive least error squares algorithm for power system relaying and measurement application", *IEEE Transactions on Power Delivery*, Vol. 6, No. 3, 1991, pp. 1008-1015.
- [7] E. Rosolowski and M. Michalik, "Fast identification of symmetrical components by use of a state observer", *IEE Proceedings - Part C: Generation, Transmission and Distribution*, Vol. 141, No. 6, November 1994, pp. 617-622.
- [8] A.A. Girgis and R.G. Brown, "Application of Kalman filter in computer relaying", *IEEE Transactions on Power Apparatus and Systems*, Vol. 100, No. 7, 1981, pp. 3387-3397.
- [9] Jyh-Cheng Gu and Sun-Li Yu, "Removal of DC offset in current and voltage signals using a novel Fourier filter algorithm", *IEEE Transactions on Power Delivery*, Vol. 15, No. 1, January 2000, pp. 73-79.
- [10] E. Rosolowski, J. Izykowski and B. Kasztenny, "A new half-cycle adaptive phasor estimator immune to the decaying DC component for digital protective relaying", in *Proceedings of the Thirty-Second Annual NAPS-2000*, Waterloo, Canada, October 23-24, 2000, pp. 2-17 - 2-24.
- [11] E. Rosolowski and J. Izykowski, "Adaptive suppressing of decaying DC component from relaying input signals", *Techniczna Elektrodynamika, Problemy Sycasnoj Elektrotehniki*, part 7, Kiev 2000, pp. 82-87.

#### VII. BIOGRAPHIES



**Waldemar Rebizant** was born in 1966 in Wroclaw, Poland. He received M.Sc. and Ph.D. degrees (both with honors) from Wroclaw University of Technology, Poland in 1991 and 1995, respectively. Since 1991 he has been a faculty member of Electrical Engineering Faculty at the WUT. In June 1996 he was awarded Siemens Promotion Prize for the best dissertation in electrical engineering in Poland in 1995. In 1999 he was granted a prestigious Humboldt research scholarship for the academic year 1999/2000. In the scope of his research interests are: digital signal processing and artificial intelligence for power system protection purposes.



**Kurt Feser** was born in 1938 in Garmisch Partenkirchen, Germany. He studied electrical engineering at the Technical University of Munich and graduated in 1963. After a year with the Brown Boveri & Cie AG in Mannheim, Germany, he joined the High Voltage Institute of the University of Munich. In 1970 he received his Dr.-Ing. from the University of Munich. And in 1971 he joined Haefely & Cie AG Basel, Switzerland, as chief development engineer for high voltage test equipment. During 1977 to 1980 Dr. Feser was member of the board of directors of American High Voltage Test Systems, Accident, Maryland. In April 1982 he joined the University of Stuttgart as head of the Power Transmission and High Voltage Institute. Prof. Feser is a Fellow of the IEEE, member of VDE and CIGRE, chairman of TC 42 "High voltage test technique" and author of more than 180 papers.



**Tammam Hayder** was born in Lattakia, Syria, in 1968. He studied Electrical Engineering at the University of Tishreen Lattakia, finishing with the Dipl.-Ing. degree in 1992. At the moment, he is Ph.D. student at University of Stuttgart, Germany, Institute of Power Transmission and High Voltage Technology (email: thayder@ieh.uni-stuttgart.de). His area of research interest is power system protection.



**Ludwig Schiel** was born in Weimar, Germany, in 1957. He studied Electrical Engineering at the Institute of Technology Zittau, finishing with the Dipl.-Ing. degree in 1984. In 1991 he received the Dr.-Ing. degree. In the same year he joined the Siemens AG, Germany, Department of Power Transmission and Distribution, Power Automation. He is project manager of transformer differential protection systems.